CrossMark

Investigation of optical properties of mixed ligand directed ZnO luminescent nanoparticles for application in light emitting diodes

Charu Narula[1] · Inderpreet Kaur[2] · Navneet Kaur[1]

Abstract Developing the heavy metal free QD-LEDs is required to curtail the risks to human beings and environment. Nanoparticles that are ecofriendly, chemically stable, easy to synthesize, nontoxic, biocompatible too are the preferred one. ZnO are biocompatible and low cost semiconductor nanoparticles with tunable band gap and large excitonic binding energy, which make them suitable for LED applications. To achieve the same purpose, this research work is focused on the synthesis of surface modified ZnO nanoparticles for their application in light emitting diodes. The condensation reaction is used to synthesize the ligand and wet chemical precipitation method is used to synthesize surface modified ZnO nanoparticles. The optical properties are evaluated using UV–Vis absorption and fluorescence studies. The optical properties are also investigated in the presence of metal ions and an increased band gap is achieved when Fe^{3+} ion is added to organic receptor coated ZnO nanoparticles. The stability of ZnO coupled receptor is confirmed theoretically using density functional theory.

1 Introduction

The development of human and environment friendly, energy saving lighting device is essential in order to sustain the energy. From many years, the various forms of lighting

✉ Navneet Kaur
navneetkaur@pu.ac.in

1 Centre for Nanoscience and Nanotechnology (UIEAST), Panjab University, Chandigarh 160014, India

2 Biomolecular Electronics and Nanotechnology Division (BEND), Central Scientific Instruments Organization (CSIO), Chandigarh 160030, India

devices are utilized including incandescent lamps and fluorescent lamps. Fluorescent lamps consume 2–5 times less power and their life is also nearly ten times more than incandescent lamps [1]. The environmental hazard issues resulting from the use of fluorescent lamps including mercury and as well to produce more efficient lighting, desires the development of light emitting diodes (LEDs). The major concern in the use of electronic devices is the power consumption [2]. In comparison to incandescent light sources, LEDs consume low energy, their life time is more, smaller in size and switching rate is faster [3, 4]. So far, these demands are mostly fulfilled by organic light emitting diodes (OLED). The recombination of electrons from cathode and holes from anode in the emissive layer made up of a film of direct wide band gap material results in the emission of light and hence depending upon the organic compound used for the fabrication of emitting layer, it emits light in the particular range of visible spectra [5]. The color emission from the organic material used in active layer is given by the difference in the energy of highest occupied molecular orbital (HOMO) and lowest unoccupied molecular orbital (LUMO) [6, 7]. To attain both pure and narrow light emission from the diode is a big confront in the field of organic light emitting diodes (OLEDs) [8, 9]. The optoelectronic device using quantum dots is becoming popular because of the low cost electronics [1]. Quantum dot LEDs (QD-LED) can be used to generate any color because these nanoparticles can emit in the entire visible range up to the infrared region simply by introducing variation in the size and chemical composition [10]. The narrow emission spectra, the broader absorption spectra, brighter emission, higher signal to noise ratio, longer lifetime, large Stokes shift and stability of QDs in comparison to organic dyes make them suitable as material in emissive layer [11]. The structure of QD-LED is

analogous to the Organic LED structure with the small difference that QD layer is inserted between electron and hole transporting materials. When a voltage is applied, electrons from the Electron transport layer (ETL) and holes from the Hole transport layer (HTL) are injected into the electroluminescent material where they recombine to form electron hole pairs, which decay to produce light emission. The QDs used in LEDs as material in active layer with different emission wavelengths and chemical compositions have shown efficient electroluminescence [12–14]. Inorganic materials show better thermal stability than organic materials [15]. A number of researchers are working on the fabrication of efficient LED with different nanomaterials [16–20]. QDs employed for efficient QD-LED are mostly based on cadmium chalcogenide semiconductors like CdSe or CdS, whose application in electronic equipment is not feasible because of environmental regulations. So far, cadmium free QD-LEDs using $CuInS_2$, InP, Si QDs have been reported; which cover the color range from green to red. Achieving blue light emission from these materials is unlikely, because particle size needs to be ultra small where stability becomes a concern. So, an increasing research effort worldwide is directed to the synthesis and application of alternative QD materials that are low cost material, easy to synthesize and which causes no threat to the environment [21]. The optical absorption, quantum efficiency, luminescence intensity and spectrum of QDs are strongly dependent on surface states [22] because the energy of the surface states lie in the band gap of the QDs [23].

ZnO being non-toxic, widely available and being vigorous against oxidation, is suitable for its use as active layer in LEDs. Its direct band gap and high exciton binding energy at room temperature enables efficient emission for LED applications in UV and visible spectral range [24]. The luminescence spectrum of ZnO nanoparticles is dominated by visible region as it shows high emission intensity in comparison to the intensity of UV region. The origin of visible emission is controversial [25]. This is owed to the surface defects and a number of acceptor and donor pairs created during synthesis. The defect and impurities result in electronic levels within the band gap which results in various electronic transitions arbitrated by these levels and thus the optical band gap energy varies [26]. The passivation of both radiative and non-radiative recombination sites on the surface of nanoparticle can be carried out by surface modification. In this research paper, the surface of ZnO nanoparticle is modified by using a capping agent that passivates the ZnO surface and also prevents it from agglomeration. The optoelectronic property of surface decorated ZnO nanoparticles is evaluated and finally a potential material is realized that can be used as luminescent active layer in light emitting devices. To the best of

our knowledge, this manuscript represents the first ZnO based imine linked biocompatible nanoparticles with tunable band gap for their application in Light emitting diodes.

2 Experimental details

2.1 Materials and methods

All the chemicals used were procured from Alfa Aesar and were of analytical grade. They were used as such without further purification. The photophysical studies were carried out by UV–Vis spectrophotometer. Specord 250 Plus Analytikjena spectrophotometer (Germany) was used to record the absorption spectra. Fluorescence measurements were performed on a Perkin Elmer LS55 Fluorescence spectrophotometer. The particle size of ZnO nanoparticles was determined using dynamic light scattering (DLS) using external probe feature of Metrohm Microtrac Ultra Nanotrac Particle Size Analyzer. ^1H NMR spectra were recorded on an Avance-II (Bruker) instrument, which operated at 400 MHz (chemical shifts are expressed in ppm). An Agilent 7700 Series ICP-mass spectrometer was used for the determination of the masses of the compounds. The morphology analysis was carried out on scanning electron microscope (SEM JEOL JSM-6610LV) using voltage of 15 kV. TEM images were recorded on a Hitachi (H-7500) instrument working at 120 kV. This instrument has a resolution of 0.36 nm (point to point) with a 40–120 kV operating voltage.

2.2 Synthesis of organic receptor

The organic receptor (R1) was synthesized using one step condensation reaction between 2-hydroxy-5-nitrobenzaldehyde (1.67 g, 10 mM) and 2aminothiophenol (1.070 ml, 10 mM) in 25 ml of methanol at room temperature for 15 h (Scheme 1). The precipitates were then filtered and the washed with methanol to get rid of impurities.

DFT calculations were made to realize the optimized structure of the receptor and also to find the band gap. The optimized structure shown in Fig. 1 has band gap of 3.1020 eV. Clearly, the HOMO densities are concentrated on S–S bond and thiophenol ring, with LUMO densities concentrated on benzaldehyde ring. The product was characterized by mass spectroscopic technique ESI–MS (Fig. 2) which shows m/z = 271.1 $[M + H]^+$, where M = $C_{26}H_{20}N_4O_6S_2$. The organic receptor was also characterized by ^1H NMR (Fig. 3). ^1H NMR (400 MHz, DMSO-d6) δ: 7.15 (d, 2H, ArH), 7.30 (m, 4H, ArH), 7.45 (d, 2H, ArH), 7.59 (d, 2H, ArH), 8.27 (dd, 2H, ArH), 8.68 (d, 2H, ArH), 9.10 (s, 2H, –CH = N), 13.5 (s, 2H, OH).
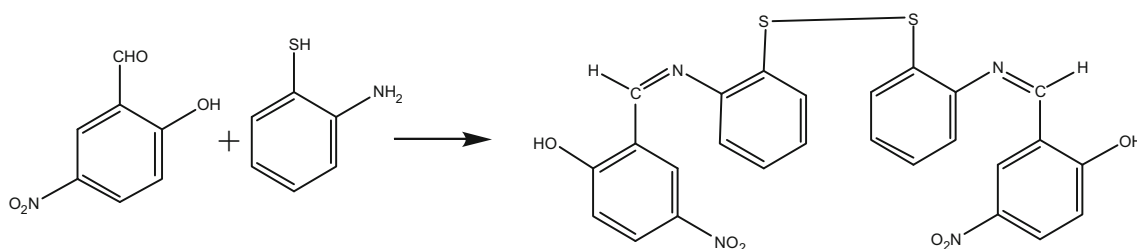
Scheme 1 Synthesis of organic receptor R1

Fig. 1 DFT optimized structure of organic receptor

HOMO (-6.204 eV)   LUMO (-3.102 eV)
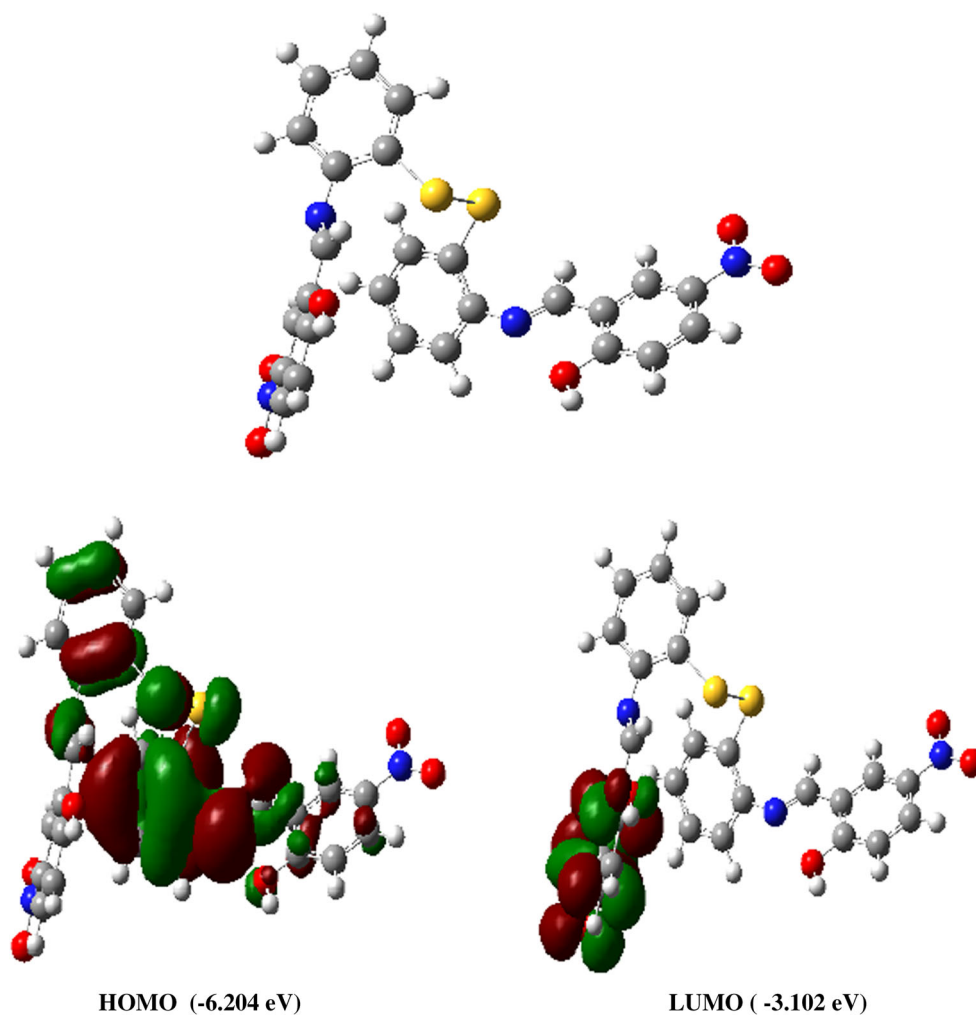
2.3 Synthesis of surface modified ZnO nanoparticles

The ZnO nanoparticles were synthesized by adding the alcoholic solution of $Zn(NO_3)_2 \cdot 6H_2O$ (0.2036 g, 0.6855 mM) to organic receptor (750 mg, 1.37 mM). 1.03 mM of NaOH in 10 ml methanol was then added drop by drop using dropping funnel. The solution was then stirred at room temperature for 24 h. A dispersion of ZnO nanoparticles was gradually formed. Yellow colored ZnO nanoparticles capped with organic receptor was then separated out upon completion of reaction and was further washed with methanol several times. The product was dried at 40 °C for 30 h. The receptor capped ZnO nanoparticles were characterized using DLS, EDX, and TEM. The structure of surface decorated ZnO nanoparticles was characterized by transmission electron microscopy (TEM). The TEM image (Fig. 4) revealed that ZnO nanoparticles are spherical in shape with size of 25 nm. The particle size was also determined using DLS, particle size analyzer, which showed size of 33 nm (Fig. 5). The
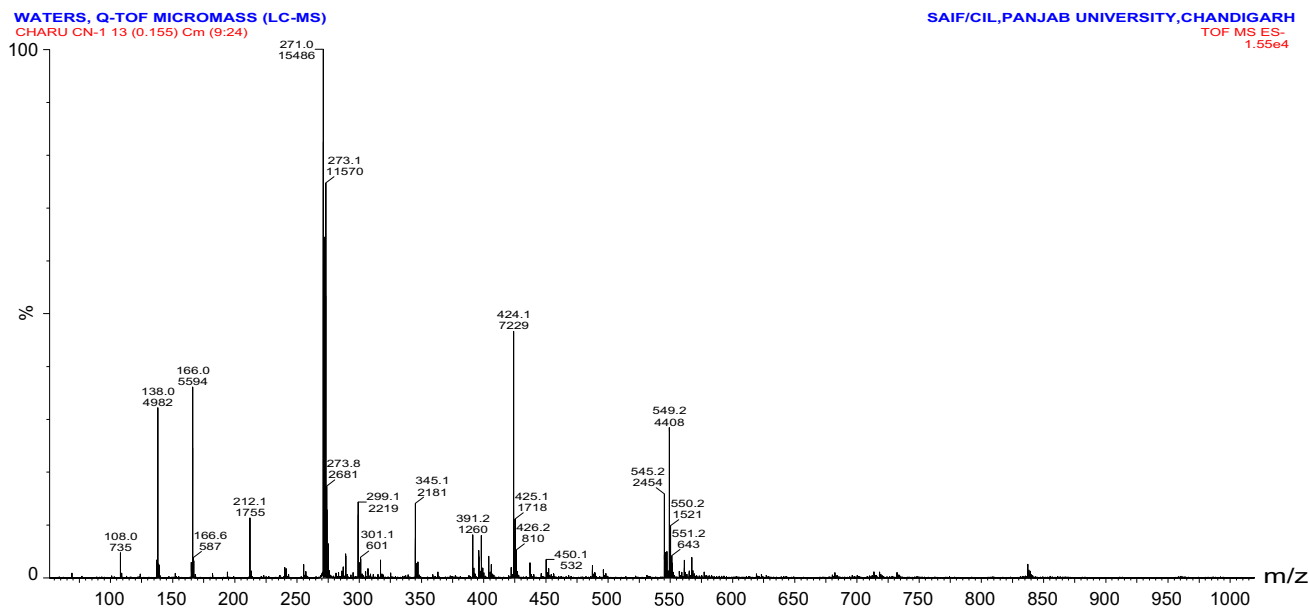
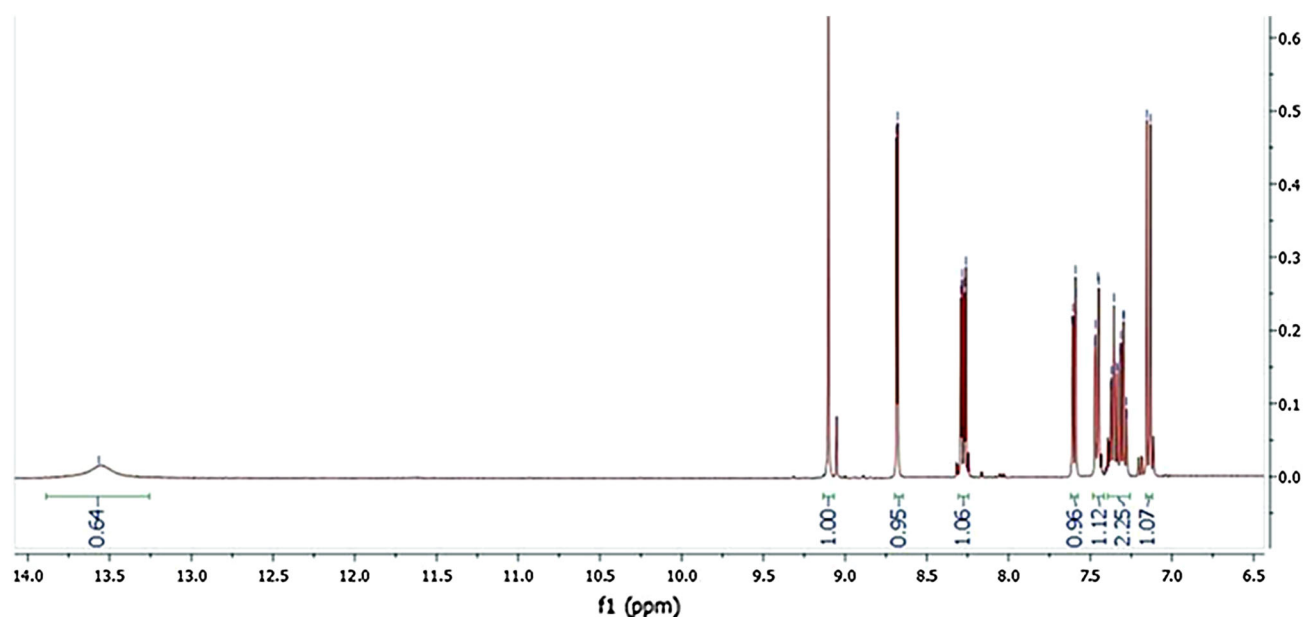**Fig. 2** Mass spectrum of organic receptor

Fig. 3 ^{1}H NMR of organic receptor

distribution of particle size of organic receptor coated ZnO nanoparticles (R1·ZnO), showing average particle size of 33 nm, was measured with DLS based particle size analyzer by dissolving the compound in DMSO: H2O (70:30; v/v). DLS is showing somewhat larger particle size as compared to TEM analysis due to hydro-dynamic radius of nano-aggregates during DLS analysis. The energy dispersive X-ray (EDX) spectrum showed the existence of organic compounds along with Zn and O, which confirmed

to the coating of organic compounds over the surface of ZnO (Fig. 6).

2.4 FTIR analyses of receptor coated ZnO nanoparticles

In FTIR spectrum, the IR transmittance signifies the characteristic of Zn–O vibration that is reliant on the particle size and morphology [27]. Series of peaks ranging
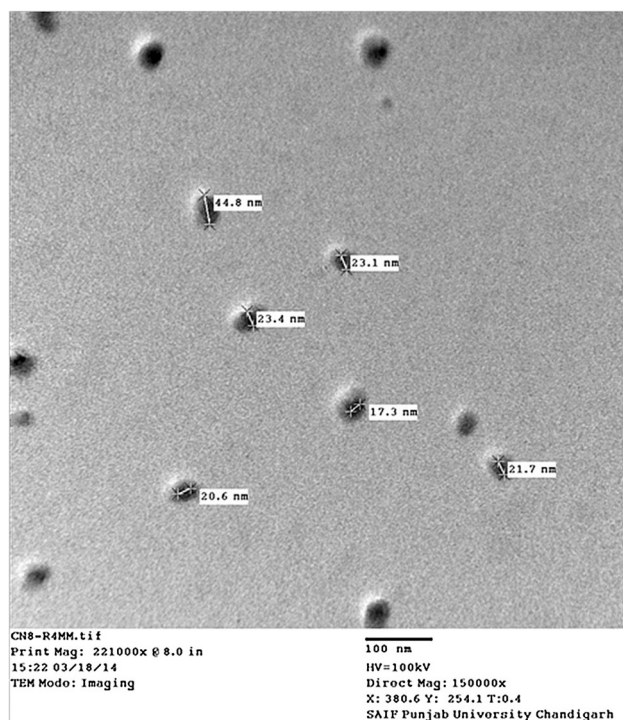
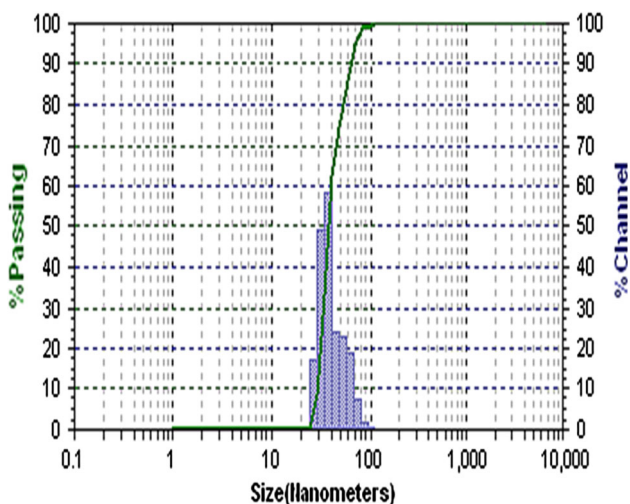Fig. 4 TEM image of R1·ZnO showing average size 25 nm

Fig. 5 DLS based particle size analyzer showing particle size of 33 nm

from 400 to 4000 cm^{-1} were found in the FTIR spectra (Fig. 7), which is due to the existence of organic groups and chemisorbed species in uncapped and receptor coated ZnO nanoparticle surface. Figure 7b shows the broad peak region between 3250 and 3500 cm^{-1} which was due to presence of stretching vibration of –OH group and amine group (N–H) on the surface of ZnO nanoparticles. The decoration of organic receptor on ZnO nanoparticle surface leads to an up field shift (shown as inset in Fig. 7). The
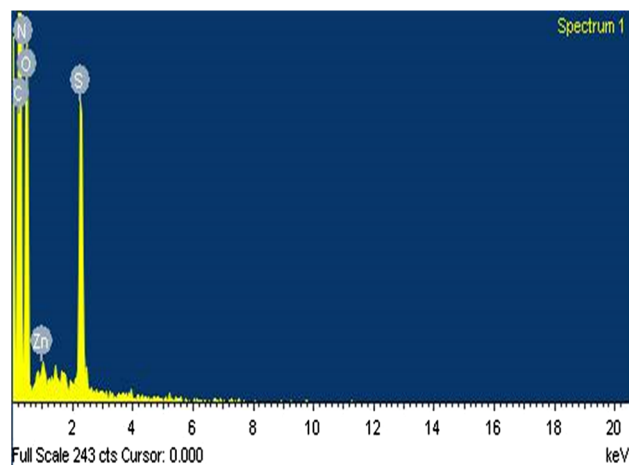

Fig. 6 EDX analysis of R1·ZnO showing the existence of organic compound together with ZnO

peak observed at 1616 cm^{-1} corresponds to stretching vibration of C=N group of the organic receptor. The presence of peaks at 1340 cm^{-1} is due to C–N stretching absorption for aromatic amines, the strong peak at 1098 cm^{-1} and 750 cm^{-1} confirmed to the bending vibrations of =C–H bond. The presence of disulphide bond is confirmed with a weak peak at 549 cm^{-1}.

2.5 DFT calculations to study the interaction of organic receptor with surface of ZnO nanoparticles

The DFT calculations were also performed to study the interaction of organic receptor with the surface of ZnO nanoparticles. The optimized organic receptor has a band gap of 3.102 eV. The ZnO nanoparticles are represented by a small cluster (ZnO)$_5$. The DFT optimized geometries of ZnO, organic receptor and (ZnO) with organic receptor shown in Fig. 8a–c respectively were obtained by using B3LYP/6-311G basis set on Gaussian 03 program. The optimized ligand represents an asymmetrical structure with both side arms perpendicular to each other. A clear change in the structure of organic receptor was noticed (Fig. 8c) when ZnO was taken along with organic ligand. The organic receptor is been attached to the ZnO ring in a symmetrical manner, where the Zn has made its bond with oxygen of hydroxy (OH) group of the ligand available in both arms. The energy of optimization also showed that a small (ZnO)$_5$ cluster with ligand has more stability as compared to isolated mixed donor ligand (Table 1).

HOMO and LUMO density of the optimized structure of ZnO with organic receptor is shown in Fig. 9. Clearly, the HOMO densities which were concentrated on S–S bond and thiophenol ring symmetrically for organic receptor, are now concentrated highly on ZnO ring after capping ZnO
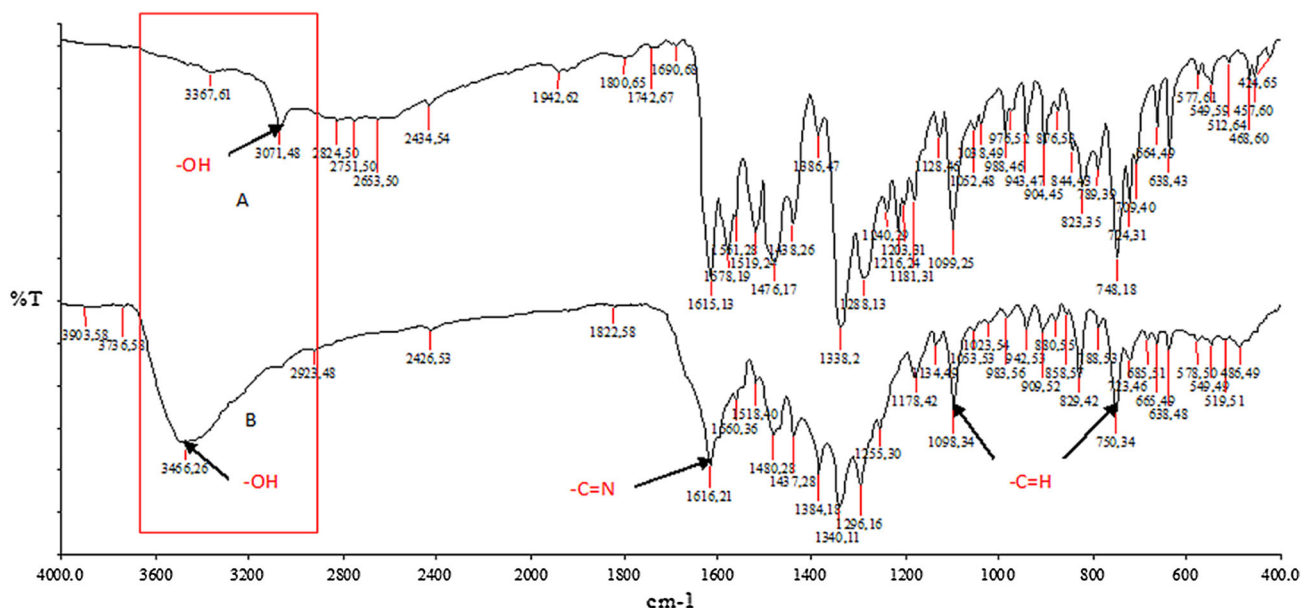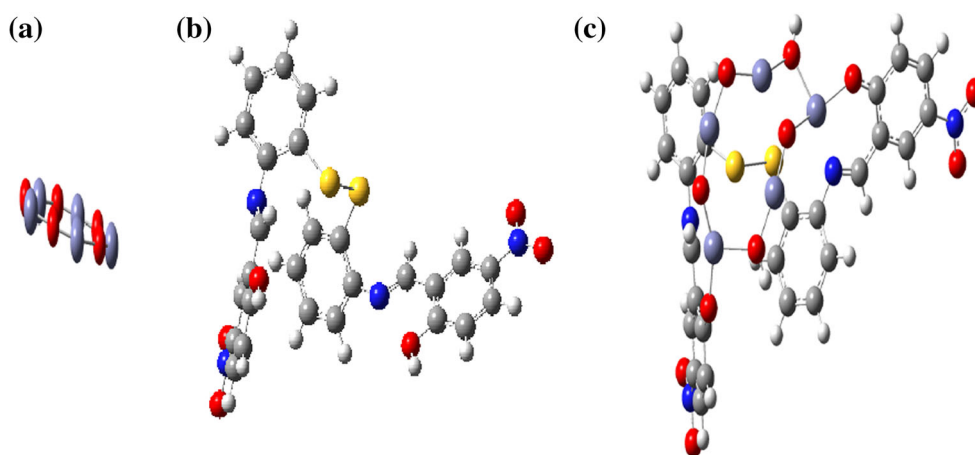
Fig. 7 *a* FTIR spectra of organic receptor and *b* An upfield shift is observed in the FTIR spectra of surface modified ZnO nanoparticles

Fig. 8 DFT optimized geometry of **a** (ZnO)₅, **b** organic receptor, **c** (ZnO)₅ with organic receptor

with organic receptor. However, the LUMO densities which were concentrated on benzaldehyde ring only for organic receptor is now symmetrically concentrated on thiophenol ring of both arms.

2.6 Photoluminescence (PL) and UV–Vis absorption studies of surface modified ZnO nanoparticles

The absorption and PL spectrum of ZnO nanoparticles was recorded to study the optical properties of capped ZnO nanoparticles. The solid state UV–Vis absorption spectrum was recorded by depositing a thin film of capped ZnO nanoparticles on the glass substrate. A comparison solid state spectra of organic receptor (ligand) and ZnO capped with receptor is shown in Fig. 10. Pure ZnO nanoparticles showed absorbance at 373 nm corresponding to exciton

state of ZnO [28], whereas the receptor capped ZnO nanoparticles in our case showed peak at 354 nm. The blue shift observed in our case is attributed to the effect of capping agents on the surface of metal oxide semiconductor nanoparticles which controlled the growth of ZnO nanoparticles immediately after the nucleation stage and thus avoided agglomeration of nanoparticles. This was so due to the layer of receptor that effectively was coated over the surface of ZnO nanoparticles. The organic receptors are good capping agents for ZnO nanoparticles, as it can efficiently passivate the surface defects and thus reduces the surface-related visible emission [29–32]. The continuity in conduction band and the valence band in case of bulk materials is changed to discrete energy levels in case of nanoparticles and thus the absorption in the (337–363) nm band may be attributed to the interband absorption taking

Table 1 The optimization parameters of ZnO, organic ligand and ZnO with ligand calculated at B3LYP/6-311G level

	Energy (a.u.)
ZnO	−9272.4
Organic receptor R1	−2468.02
ZnO with organic receptor (R1·ZnO)	−11,741.06

place between the conduction and valence band. The band gap of surface modified ZnO nanoparticles was also calculated using Tauc plot (Fig. 11). The band gap of pure ZnO nanoparticles is 3.37 eV [33], whereas increased band gap was observed in our case because of the quantization of energy states with the decrease in the size of nanoparticles. In the present study, the receptor was used as a capping agent which controls the growth of ZnO nanoparticles immediately after the nucleation stage and thus the agglomeration is avoided. The ZnO nanoparticles synthesized were of average size 25 nm approximately with size ranging from 17 to 37 nm. The band gap of any material is its size dependent property. As the size of nanoparticle reduces, the increase in the band gap is observed. We have calculated the band gap of receptor capped ZnO nanoparticles from its molar absorptivity obtained from UV–Vis spectroscopic analysis. The coated ZnO nanoparticles was investigated by calculating band gap (E), using Tauc plot Equation given below:

$$Ah\nu = A\left(h\nu - E_g\right)^{1/2},$$

where A is the absorbance, h is the Planck's constant, ν is the frequency and E_g is the band gap. The band gap observed in the case of surface modified ZnO nanoparticles is 3.9 eV. An increase in the band gap observed is also an indication of reduction in the size of ZnO nanoparticles. An approximate band gap range from (3.4–3.9) eV was observed because of different particle size of synthesized
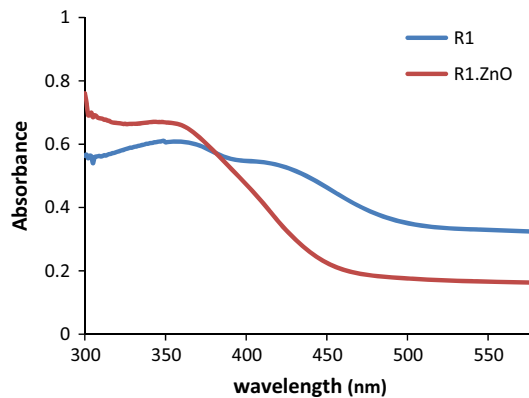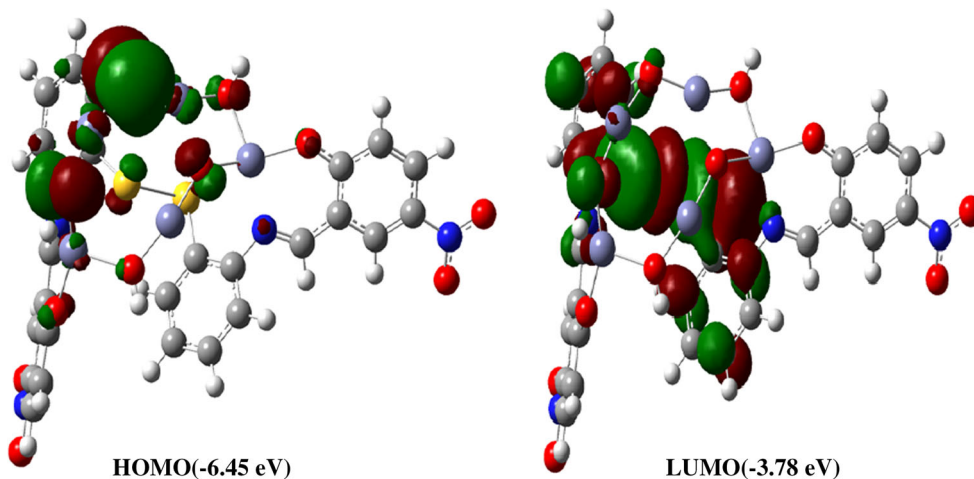

Fig. 10 Comparison of solid state UV–Vis spectra of organic receptor R1 and ZnO capped with receptor R1·ZnO
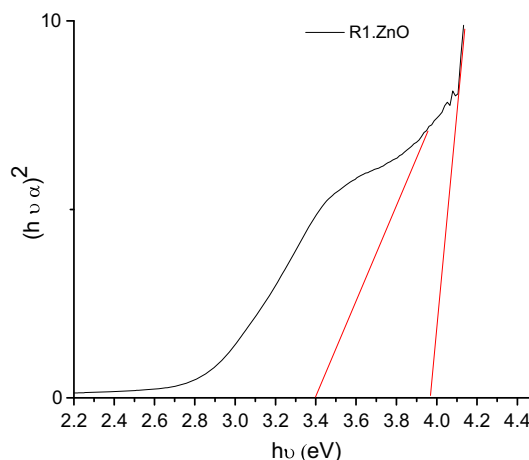

Fig. 11 Band gap of surface modified ZnO nanoparticles showing band gap of 3.9 eV using Tauc plot

ZnO nanoparticles. The increase in the band gap observed in the present study thus requires an extra energy to extract an electron from the valence band to the conduction band,

Fig. 9 HOMO and LUMO densities of (ZnO)₅ with organic receptor

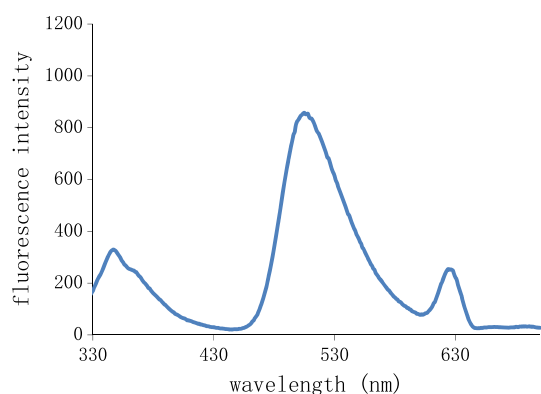**HOMO(-6.45 eV)**   **LUMO(-3.78 eV)**

Fig. 12 PL spectra of receptor coated ZnO nanoparticles (R1·ZnO)

and hence the synthesized material finds its application in lasers and LEDs.

The photoluminescence studies were done for surface modified ZnO nanoparticles. The PL spectra for receptor capped ZnO nanoparticle was recorded in the range of 330 nm–700 m. A sharp peak was observed at 500 nm (Fig. 12). The emission at 500 nm for capped ZnO nanoparticles resulted in fluorescence in coated ZnO nanoparticles. The bluish green emission in the visible range was observed.

The influence of metal ion on the receptor capped ZnO nanoparticles is carried out to observe if any change occurs in the optoelectronic properties and the change in the absorption profile of ZnO nanoparticles is practiced upon addition of a particular metal nitrate salt as the photophysical properties of the fluorescent chemosensors changes upon its interaction with the chemical species in such a way that its fluorescent signatures are observed [34]. All the recognition studies were carried out at 25 ± 1 °C, and before recording any spectrum, sufficient time was given for shaking to ensure the uniformity of the solution. The metal nitrate salts of different cations were added to the compound R1. ZnO to study the effect of the presence of different cations, including Li^+, Na^+, K^+, Mg^{+2}, Ca^{2+}, Sr^{2+}, Ba^{3+}, Cr^{3+}, Mn^{2+}, Co^{2+}, Zn^{2+}, Ag^+, Cd^{2+}, Hg^{2+}, Pb^{2+}, Cs^{2+} and Al^{3+}, on ZnO coated with receptor through the changes in absorption spectra of R1·ZnO (Fig. 13). The metal binding test was carried out by mixing standard solutions of the sensor R1·ZnO (5 ml) along with fixed amounts of a particular metal nitrate salt [50 μM in HEPES-buffered in DMSO/H_2O (7:3, v/v)]. The changes in the UV–Vis absorption spectrum were recorded to monitor any change in the absorption profile of R1·ZnO (host) in presence of the metal nitrate salts. The absorption spectra (centered at 354 nm) of host has not shown any significant change with most of the metal ions tested, however the addition of Fe^{3+}, Al^{3+} and Cu^{2+} resulted in the blue shift in absorption spectra The blue shift caused by the addition of
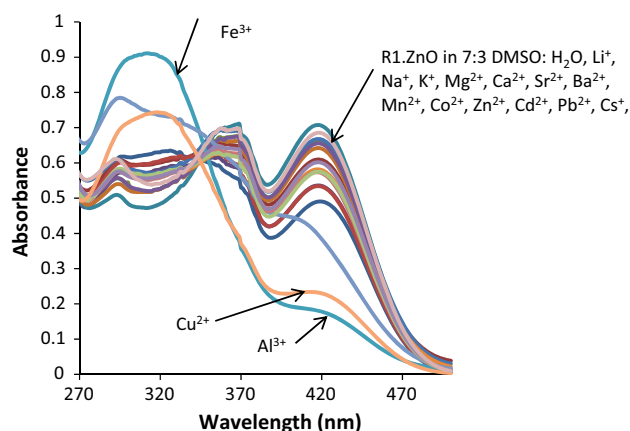

Fig. 13 Changes in the UV–Vis spectrum of R1·ZnO upon addition of 5 equivalent of metal nitrate salts
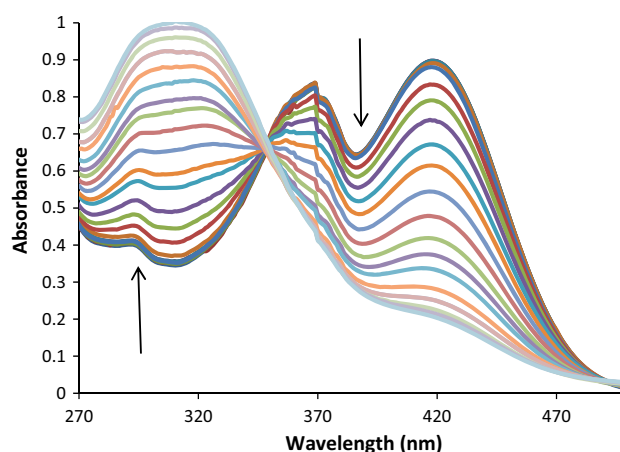

Fig. 14 Changes in the UV–Vis spectrum of R1·ZnO (10 μM) in the presence of different concentrations of Fe^{3+} (0–100 μM)

cation in R1·ZnO conjugate resulted in the increase in the band gap. The absorption spectra is blueshifted at 310 nm with Fe^{3+}. This tunable band gap achieved in this case can be utilized in OLEDs.

To further investigate the ability of the capped ZnO nanoparticles (R1·ZnO) to bind selectively with Fe^{3+}, titrations were carried out by adding small aliquots of Fe^{3+} and changes were observed using UV–Vis absorption spectroscopy (Fig. 14). The successive addition of Fe^{3+} ions (0–100 μM) to the host solution (10 μM) confirmed to the changes observed during the metal binding tests with the isosbestic point at 349 nm. The receptor itself was checked for the metal binding studies with the metal nitrate salts but the ligand showed no selectivity for any of the metal ion. The ZnO based imine linked biocompatible nanoparticles functionalized with Fe^{3+} with tunable band gap can find their application as emissive layer in light emitting diodes. This material is proposed as a probable

material for active layer in LEDs, being safe, biocompatible, nontoxic considering environmental issues. So, pure and narrow line emission can be achieved with this proposed material.

3 Conclusion

The optical properties of organic receptor directed ZnO luminescent nanoparticles were investigated for their application in light emitting diodes. The photophysical studies were carried out for receptor coated ZnO nanoparticles which demonstrated the absorption at 354 nm and emission at 500 nm. The photophysical studies were further investigated for ZnO nanoparticles capped with organic receptor in the presence of metal ion, and thus in the presence of Fe^{3+}, the absorption spectra was found to get blue shifted at 310 nm, resulted in tunable band gap. This tunable band gap achieved with receptor capped ZnO nanoparticles and receptor capped ZnO in presence of metal ion can be well utilized for light emitting diodes.

References

1. T.H. Kim, W. Wang, Q. Li, Front. Chem. Sci. Eng. (2012). doi:10.1007/s11705-011-1168-y
2. K. Bazaka, M.V. Jacob, Electronics **2**, 1–34 (2013)
3. K.H. Chan, Architect. Eng. Des. Manag. **8**, 21–29 (2012)
4. D. Wood, *Joint Cognitive Systems* (CRC Press, USA, 2006)
5. Y. Karzazi, J. Mater. Environ. Sci. **5**(1), 1–12 (2014)
6. W.L. Yu, Y. Cao, J. Pei, W. Huang, A.J. Heeger, Appl. Phys. Lett. **75**(21), 3270–3272 (1999)
7. B.W. D'Andrade, R.J. Holmes, S.R. Forrest, Adv. Mater. **16**, 624–628 (2004)
8. V.K. Khanna, *Fundamentals of Solid State Lighting: LEDs, OLEDs and their Applications in Illumination and Displays* (CRC Press, USA, 2014)
9. S.W. Sanderson, K.L. Simons, Res. Policy **43**, 1730–1746 (2014)
10. D. Bera, L. Qian, T.K. Tseng, P.H. Holloway, Materials **3**, 2260–2345 (2010)
11. U.R. Genger, M. Grabolle, S.C. Jaricot, R. Nitschke, T. Nann, Nat. Methods **5**, 763–775 (2008)
12. S. Coe, W.K. Woo, M.G. Bawendi, V. Bulovic, Nature **420**, 800–803 (2002)
13. J.S. Steckel, W.K. Woo, M.G. Bawendi, V. Bulovic, Angew. Chem. Int. Ed. Engl. **45**, 5796–5799 (2006)
14. L. Kim, P.O. Anikeeva, S.A. Coe-Sullivan, J.S. Steckel, M.G. Bawendi, V. Bulovic, Nano Lett. **8**, 4513 (2008)
15. J.W. Gilman, Appl. Clay Sci. **15**, 31–49 (1999)
16. S. Bera, S.B. Singh, S.K. Ray, J. Solid State Chem. **189**, 75–79 (2012)
17. T.D. Hoanh, Y.H. Im, D.E. Kim, Y.S. Kwon, B.J. Lee, J. Nanomater. (2012). doi:10.1155/2012/451306
18. S. Bhaumik, A.J. Pal, IEEE J. Quantum Electron. **49**, 325–330 (2013)
19. C. Ippen, T. Greco, Y. Kim, J. Kim, M.S. Oh, C.J. Han, A. Wedel, Org. Electron. **15**, 126–131 (2014)
20. J. Chen, D. Zhao, C. Li, F. Xu, W. Lei, L. Sun, A. Nathan, X. W. Sun, Sci. Rep. **4**, 4085. (2014). doi: 10.1038/srep04085
21. E.Q. Contreras, M. Cho, H. Zhu, H.L. Puppala, G. Escalera, W. Zhong, V.L. Colvin, Environ. Sci. Technol. **47**(2), 1148–1154 (2013)
22. D.M. Yeh, C.F. Huang, Y.C. Lu, C.C. Yang, Appl. Phys. Lett. **92**, 1–3 (2008)
23. E. Kucur, W. Bucking, R. Giernoth, T. Nann, J. Phys. Chem. B **109**, 20355–20360 (2005)
24. E. Neshataeva, T. Kummell, G. Bacher, A. Ebbers, Appl. Phys. Lett. **94**, 091115 (2009)
25. A.V. Dijken, E.A. Meulenkamp, D. Vanmaekelbergh, A. Meijerink, J. Phys. Chem. B **104**, 1715–1723 (2000)
26. M. Šćepanović, M. Grujić-Brojčin, Z. Dohčević-Mitrović, Z.V. Popović, J. Phys. Conf. Ser. **253**, 012015 (2010)
27. K.M. Kim, M.H. Choi, J.K. Lee, J. Jeong, Y.R. Kim, M.K. Kim, S.M. Paek, J.M. Oh, Int. J. Nanomed. **9**(Suppl 2), 41–56 (2014)
28. S. Kaur, A. Kaur, N. Kaur, Mater. Lett. **100**, 19 (2013)
29. S. Tachikawa, A. Noguchi, T. Tsuge, M. Hara, O. Odawara, H. Wada, Materials **4**, 1132–1143 (2011)
30. C. Narula, I. Kaur, N. Kaur, J. Mater. Sci. Mater. Electron. **26**, 791–800 (2015)
31. S. Gulia, R. Kakkar, Adv. Mater. Lett. **4**(12), 876–887 (2013)
32. H. Sharma, A. Singh, N. Kaur, N. Singh, ACS Sustain. Chem. Eng. **1**, 1600–1608 (2013)
33. S.C. Lin, Y.L. Lee, C.H. Chang, Y.J. Chen, Y.M. Yang, Appl. Phys. Lett. **90**, 143517-(1-3) (2007)
34. A. Saini, J. Singh, R. Kaur, N. Singh, N. Kaur, New J. Chem. **38**, 4580 (2014)